ISSN 1063-7710, Acoustical Physics, 2018, Vol. 64, No. 6, pp. 718–730. © Pleiades Publishing, Ltd., 2018.
Original Russian Text © S.Yu. Krasheninnikov, A.K. Mironov, L.A. Benderskii, 2018, published in Akusticheskii Zhurnal, 2018, Vol. 64, No. 6, pp. 704–717.

ATMOSPHERIC AND AEROACOUSTICS

Analysis of Noise Generation by Turbulent Jets from Consideration of Their Near Acoustic Field

S. Yu. Krasheninnikov[a], *, A. K. Mironov[a], and L. A. Benderskii[a]

[a] *Central Institute of Aviation Motors, Moscow, 111116 Russia*

* *e-mail: krashenin@ciam.ru*

Received March 7, 2018

Abstract—The paper studies the generation of acoustic waves near the boundaries of swirling and nonswirling turbulent jets outside a jet flow. Nonstationary motion of the medium is analyzed. In the case of swirling jets, the occurrence and propagation of perturbations were studied experimentally, while in the case of free turbulent jets, both experimentally and numerically on the basis of LES technology. The results of the study show that, near the jet boundaries, there is a region in which the phase difference between pressure and velocity pulsations at fixed frequencies is 90° or more; i.e., there are no perturbations propagating outward. The phases of velocity and pressure pulsations coincide starting from some significant distance from the jet boundaries. The region in which the phase difference varies from 90° to 0° lies outside the jet flow and is presumably the sound generation region. It is proposed that this region be identified with the near acoustic field of jets.

Keywords: turbulent jets, swirling jets, induced flow, pressure pulsations, intermittency, noise generation, acoustic waves, occurrence of depression in a jet

DOI: 10.1134/S1063771018060076

INTRODUCTION

Free turbulent jets produce perturbations in the surrounding medium, which at some distance from the jet are perceived as acoustic waves. These perturbations are caused by the nonstationary pulsating motion of the medium in the jet flow [1].

It should be noted that, in experimental studies of the noise generation process in turbulent jets, a number of contradictory facts have been established.

On the one hand, the noise spectrum of a free turbulent jet is uniform and does not contain the selected frequencies. Analyses of the pulsation characteristics of the flow in a turbulent jet do not reveal the characteristic frequencies in pulsations of the velocity, pressure, and other parameters.

Measurements of the correlation coefficients for pulsations of parameters in a jet and acoustic pulsations show that they are on the order of 10^{-3}.

On the other hand, from numerous experimental data on the location of noise sources in a fixed frequency band, it is possible to obtain a definite relation between the frequency of the emitted noise and the position of the noise source of a given frequency in the jet mixing layer.

Such data indicate the existence of periodic processes in hydrodynamic pulsations accompanied by noise generation, which is observed at a distance from turbulent jets.

However, the assumptions made from such observations about the presence of coherent structures in a jet have not been confirmed. The difficulty of revealing periodic processes in a turbulent flow is apparently related to the general instability of the flow in the mixing layer of a turbulent jet.

Hence follows the assumption that it is the instability of the flow in the jet mixing layer that manifests itself as the intermittency in turbulence, which, on the one hand, causes a certain quasi-periodicity in the turbulent flow and, on the other, makes it difficult to distinguish periodic processes in experiments because of their randomness. These dual properties of intermittency, in turn, are manifested in the observed correspondence between the characteristic frequencies of the emitted noise and the location of the sources determined in the experiments. This is confirmed by the results of joint measurement of the characteristic scales of intermittent inhomogeneities in the jet mixing layer and the frequency components of the jet noise.

According to the results of experiments, acoustic radiation by a turbulent jet is formed due to the motion of dynamic inhomogeneities whose characteristic scale exceeds the thickness of the mixing layer by almost half in each characteristic section of the mixing

layer. These large-scale formations are caused by the intermittency in turbulence. Thus, to analyze the noise generation process in a turbulent jet, it is necessary to reveal the occurrence of "almost periodic" perturbations in the nonstationary turbulent flow in the jet mixing layer and its vicinity.

From the viewpoint of analyzing the noise generation process, it is easier to study the noise of a swirling jet. The noise of strongly swirling jets is tonal and narrowband. It is produced by the precessional motion in the jet flow. This facilitates experimental study of the acoustic radiation process.

In this study, we analyze the generation of acoustic waves as a result of nonstationary flow dynamics in turbulent swirling and nonswirling jets and illustrate the transient process of transformation of hydrodynamic pulsations into acoustic ones.

For this purpose, joint measurements of pressure and velocity pulsations were performed inside and outside a jet flow. In swirling jets, the velocity component distributions in the jet flow and its neighborhood are measured using PIV technology. The static pressure distribution in free turbulent jets was measured.

Numerical modeling of nonstationary processes in turbulent jets was performed with LES technology. Data on the flow parameters accumulated in nonstationary calculations were processed. From these data, the instantaneous, averaged, and time-dependent flow parameters were determined. The propagation of perturbations was also studied using Fourier analysis with the identification of specific frequencies of pulsations. For the phase characteristics of pulsations in a free turbulent jet, the data obtained for several cross sections of the jet at a flow velocity of 310 m/s are presented. The data obtained for a velocity of 200 m/s and in other sections are consistent with them.

The data obtained show that the propagation of turbulent jets is accompanied by the formation of large-scale depression regions, the motion of which exhibits periodicity.

In intensely swirling jets, this periodicity arises due to the precessional motion with the rotation of a nonuniform parameter distribution in the jet cross section. The rotation of the depressed region causes a periodic transformation of the inflow from the surrounding medium to the jet. The frequency of this periodic process is equal to the frequency of the tonal noise of the jet.

In the case of free turbulent jets, the motion of the depressed regions arising in the jet mixing layer is observed. The reduction in the static pressure in these regions reaches 20% of the jet velocity head. These regions induce inflow to the jet. The succession of motion of these regions in the cross sections of the jet is close to periodic. Consequently, in the surrounding medium, periodic rearrangement—pulsations in the induced inflow—arises near any cross section of the jet. Since the size of the depressed regions increases along the jet, the characteristic frequencies of pulsations arising in the ejected flow decrease. Their dependence on the longitudinal coordinate corresponds to the data on the frequencies of the noise emitted by different sections of the jet.

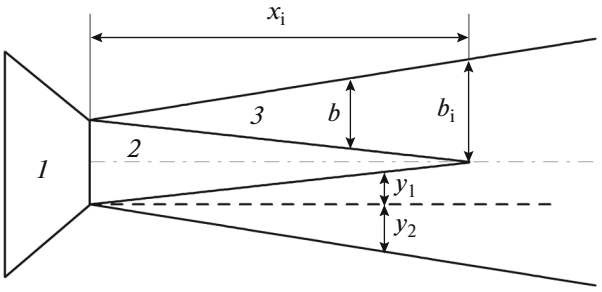

Fig. 1. Flow pattern in turbulent jet, initial section: (*1*) nozzle, (*2*) "core" of jet, and (*3*) mixing layer. Index "i" corresponds to end of initial section.

In general, the results of this study confirm our earlier hypothesis on the noise generation mechanism in turbulent and swirling jets. It is assumed that the noise generation process is caused by quasi-periodic pulsations observed near the boundaries in the inflow to the jet.

The inflow to the jet is nonstationary and is induced by the intermittent motion of regions with reduced static pressure in the jet flow. The nonstationary processes taking place in the inflow are observed in the immediate vicinity of the jet boundaries. In other words, the so-called near acoustic field of the jet can be the source of noise from turbulent jets.

SPECIFICS OF THE FLOW STRUCTURE IN JETS RELATED TO THE MANIFESTATION OF LARGE-SCALE NONSTATIONARITY

Investigations of the structure of jet flows make it possible to adopt the scheme of the flow in a turbulent jet proposed in [2, 3].

Figure 1 shows the flow pattern in its initial section (see Fig. 1.2.1 from [3]).

The conditional boundaries of the mixing zone enclosed between the boundaries $y_1 = 0.11x$ and $y_2 = 0.16x$ are shown. The x-coordinate is calculated from the nozzle edge. Between these boundaries, there is a mixing layer with a width of $b \approx 0.27x$. (Below, in separate figures, these boundaries are shown by dashed lines.)

According to the general concepts, in particular, set forth in [1, 4–6], acoustic radiation is generated in this mixing layer, where the most intense turbulent pulsations and a high level of vorticity are observed. In many known studies, e.g., [7–12], various elements of turbulent flows are considered possible noise generation sources: in [7], intermittency in turbulence; in [8–10], structural elements of turbulence; and, in [11, 12], instability waves and coherent structures.

However, there are experimental data showing that the sound sources are located beyond the region of the jet flow [13–15]. In addition, the well-known fact [5, 16] of single-valued dependence of the acoustomechanical efficiency of turbulent jets on the ratio of the jet flow velocity to the speed of sound in the surrounding medium, i.e., on the acoustic Mach number M_a, also speaks to the defining role of the properties of the surrounding medium in the sound generation process.

The determination of sound sources in jets can be facilitated by revealing in them periodic hydrodynamic processes. The feasibility of this approach to swirling jets emitting a tonal noise is obvious. The data on noise generation in turbulent jets also make possible this approach.

In [7], a work devoted to an experimental study of the combined characteristics of the acoustic field and the structure of the turbulent flow in the mixing layer, a relation between the features of turbulent pulsation motion and noise emission was demonstrated. In this work, as well as in earlier studies of other authors [6, 17–19], a relationship between the frequency of radiation and the distance from the origin of the mixing layer (nozzle edge), at which radiation at a given frequency is detected, was confirmed.

The results of conditional phase averaging of PIV data for transverse acoustic excitation of an axisymmetric jet for the propagation of instability waves [20] showed good agreement with the known data on the localization of sound sources at the characteristic frequencies.

These experiments, conducted in a wide variety of conditions, show that there is a relationship between the longitudinal coordinate of the source and the characteristic frequency of sound radiation. This relationship for the initial section of the jet is expressed approximately as

$$\mathrm{Sh}_d = \frac{fd}{u_0} = 1.55\frac{d}{x}. \quad (1)$$

Here, f is the radiation frequency, d is the diameter of the nozzle from which the jet propagates, u_0 is the jet velocity, and x is the longitudinal coordinate calculated from the nozzle edge.

Investigations carried out in [7] showed that, in the middle part of the mixing layer, at a given point of the flow, a quasi-periodic passage of inhomogeneities takes place, detected by thermoanemometric measurements. If the characteristic size of these inhomogeneities is L, the period of their motion is $T = L/u_c$ and the repetition frequency is

$$f_c = \frac{1}{T} = \frac{u_c}{L}. \quad (2)$$

Here, u_c is the velocity of the motion of inhomogeneities. This inhomogeneity can be identified by thermoanemometric measurements of turbulence. The inhomogeneities under consideration move in the flow with the so-called convection velocity u_c, and their size is proportional to x.

According to the results of measurements in the middle part of the mixing layer (at the level of the nozzle edge), the convection velocity of vortices is

$$u_c \cong 0.5–0.6u_0.$$

In this case, the acoustic perturbation frequency obeys relation (1):

$$f = 0.7u_c/b.$$

As a result, we obtain the relation between the acoustic radiation wavelength λ and the scale of the inhomogeneity of the turbulent flow:

$$\lambda = \frac{\alpha L}{u_c} = \frac{L}{M_c} \approx 2\frac{L}{M_a}. \quad (3)$$

The size of the inhomogeneity of the turbulence in the mixing layer was found to be

$$L \cong 0.385x. \quad (4)$$

The observed noise spectrum of a turbulent jet is "continuous", without separate tones. The available data on measurement of the correlation coefficients between acoustic pulsations outside the jet and various pulsations in the jet [21, 22] indicate their independence. However, the data described above lead to the conclusion that the noise of free turbulent jets consists of some periodic processes, although they have a significant element of randomness.

An example of a definite relationship between periodic purely hydrodynamic perturbations and radiated noise is noise generation in swirling jets [23, 24]. In these studies, the pronounced tonality of the noise of swirling jets was used to establish the relation between the noise emitted by the jets and the nonstationary processes in them. In this case, phase measurements can be carried out rather easily and, with their help , the basic properties of both jet flows and acoustic radiation can be determined.

In other words, when studying free turbulent jets, revealing the periodic processes and their properties can help in determining the characteristics of the noise generation process and the location of noise sources.

In this work, we analyze periodic processes near the boundaries of jet flows and establish their relationship with acoustic wave generation.

In a number of works [13–15, 23, 24] in which the formation of acoustic perturbation near the boundaries of swirling and nonswirling turbulent jets was analyzed from experiments and numerical calculations, it was established that acoustic perturbations propagating from the jet are produced beyond their usually adopted boundaries, i.e., beyond the boundaries that encompass the region of turbulent flow. For a free turbulent jet, an example of such a boundary is the line $y_2 = 0.16x$ (shown in Fig. 1).

In this study, to analyze the processes associated with noise generation of turbulent jets, the pulsation parameters of the flow in jets and near their boundaries are analyzed.

At some distance from the jets, the perturbations produced by them are perceived in the surrounding medium as acoustic waves. As for the initial perturbations, they are a consequence of nonstationary processes in jets: turbulence, intermittency in turbulence, and the precessional motion in swirling jets. In other words, there is a mechanism by which nonstationary processes in jets affect the surrounding medium, which leads an increase in acoustic waves. We can assume the following succession of elements of these processes: nonstationary motion in the jet; its effect on the nearest vicinity of the jet, where it gives rise to a nonstationary motion in the external flow; and the formation of an acoustic energy flux and acoustic field.

The objective of this study was to determine the role of the so-called near field of the jet in this process. The existing concepts for determining its boundaries were set forth in [4] as follows: in the near acoustic field, the phases of velocity and pressure pulsations do not coincide due to the presence of hydrodynamic pulsations, which vanish beyond near field; the boundaries of the near field are determined by the completion of this process; the distance of these boundaries from the generally accepted boundaries of the jet also depends on the frequency of pulsations under consideration, i.e., the jet velocity.

As a result of this study, other ideas on the near field are justified. According to the data obtained, the acoustic radiation observed in the far field at large distances from the jet can be generated in the immediate vicinity of the jet boundaries in the surrounding medium. In other words, hydrodynamic pulsations observed in the near field can lead to the generation of a flux of radiated acoustic energy. This, in turn, agrees with the decisive role for the acoustic characteristics of a jet with the acoustic Mach number calculated from the efflux velocity and the speed of sound in the surrounding medium, $M_a = u/a$.

Since the acoustic radiation of an ordinary turbulent jet is broadband and there are difficulties in carrying out phase analysis of propagating perturbations, to study the properties of acoustic radiation produced by jets, we additionally used the results of experiments with swirling jets [23, 24]. The noise of such jets is emitted at fixed frequencies, which facilitates the experiments.

INVESTIGATION OF NONSTATIONARY PROCESSES IN JETS AND NEAR THEIR BOUNDARIES

The acoustic radiation from an ordinary turbulent jet is broadband, which made it difficult to conduct phase analysis experiments. Therefore, we used computer simulation of a turbulent flow in a jet, the method and separate results of which are given in [14, 25]. We also used experimental results concerning the relation between the characteristics of a turbulent flow in the jet mixing layer and the noise emitted by it [7], which were obtained in a study of sound generation in a free turbulent jet.

As mentioned above, in accordance with data on the location of noise sources for a fixed frequency and the results of measuring the convection velocity of vortices of different scales, it was concluded that there is a relation between the longitudinal scale of an inhomogeneity moving in the mixing layer with convection velocity u_c and wavelength λ (3) of the acoustic perturbation produced.

According to the measurements in [7], which are generalized in relations (1)–(4), the dynamic inhomogeneities the motion of which is caused by pulsations outside the jet, have a longitudinal dimension L exceeding the mixing layer width b in the corresponding section of the jet:

$$L \cong 0.385x = 1.425b. \quad (5)$$

Thus, according to [7], L is the characteristic scale of inhomogeneities producing the initial perturbations at frequency $f = u_c/L$, which corresponds to the radiated acoustic waves.

The calculation data make possible an addition test of this result. Turbulent jets propagating from a nozzle with a diameter $d = 2$ m with a subsonic efflux velocity of about 200 and 310 m/s were calculated. The LES technology described in [14, 26] was used. The representativeness of the numerical results is confirmed by an almost exact match of the averaged flow structure with the known data (see Fig. 1) and agreement between the characteristic sizes of dynamic inhomogeneities obtained in calculations and in experiments [7]. In addition, the calculated characteristics of the acoustic field of the jet determined from numerical calculations agree in the spectrum, radiation pattern, and sound pressure level with the data of [25].

Figure 2 shows the flow structure in the mixing layer of a free turbulent jet obtained in calculations. The instantaneous static pressure field in the plane of symmetry is shown. The coordinate $y/d = 0.5$ corresponds to the nozzle edge and the middle part of the mixing layer. Light areas correspond to pressure above atmospheric, and dark areas correspond to depression. Streamlines are also given. The calculated averaged values of the flow parameters show that they agree well with the known data on the averaged flow structure in jets. According to the approximation of the calculated data, the thickness of the mixing layer and the position of its boundaries correspond to Fig. 1.

Figure 3 shows the static pressure minus the atmospheric pressure in the instantaneous distributions shown in Fig. 2, obtained from the results of calculations and measurements in [26]. The difference in

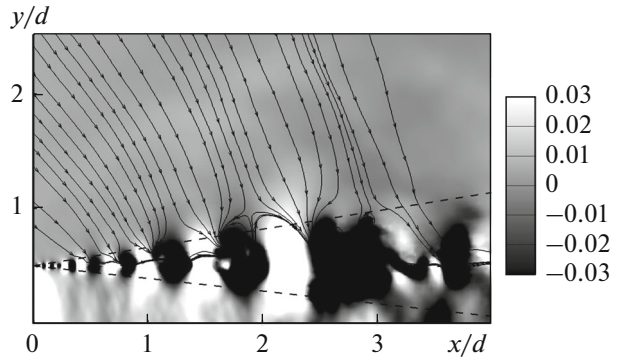

Fig. 2. Results of calculating instantaneous distribution of static pressure in mixing layer and streamlines in ejected flow.

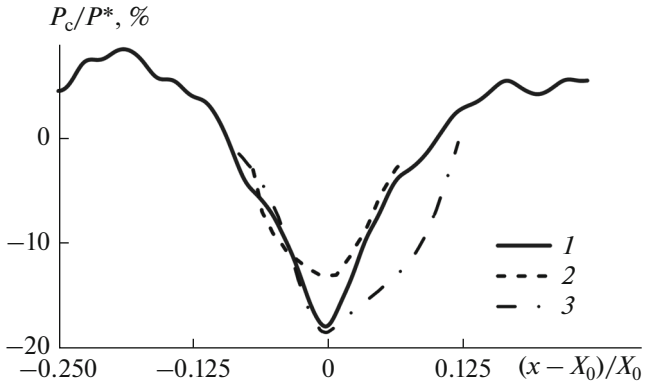

Fig. 3. Instantaneous values of static pressure within one inhomogeneity of static pressure distribution: (*1*) experiment and (*2, 3*) calculations for u_0 = (*2*) 200 and (*3*) 310 m/s. P^* is velocity head at nozzle cut.

static pressure and the external pressure is related to the jet velocity head and is represented as the dependence on the similarity coordinate $(x - X_0)/X_0$ (where X_0 is the coordinate of the minimum pressure value), displaced in the longitudinal direction. In Fig. 3, it is quite clear that the data obtained are in good agreement with empirical relation (4).

The data in Fig. 3 show that, in depressed regions, the depression amounts to 20% of the jet velocity head. The mean pressure on the line continuing the nozzle edge corresponds to a depression of ~4% of the jet velocity head [26]. This reduction in the static pressure induces an inflow of the surrounding medium into the jet, the streamlines of which are shown in Fig. 2. The data from calculating the static pressure in jets have been confirmed experimentally in [26].

Figure 4 shows the instantaneous flow patterns with the selection of streamlines in the flow induced by the jet in the surrounding medium. The visualization is the same as in Fig. 2. Figure 4a shows the distribution of the parameters at a certain initial time; and Figs. 4b–4d, at subsequent time instants with a step of 0.0016 s of physical time, as well as a small selected area of the external flow. It can be seen that external streamlines are entrained by depressed regions and, as a result, reciprocate.

In the analysis of the motion of streamlines, manifestation of periodicity is observed. Groups of several streamlines following the moving depression regions return to their initial positions. The observed reciprocal motion of streamlines has a period which, according to (2), corresponds to the characteristic radiation frequency for a given distance from the nozzle edge:

$$T = \frac{1}{f} \cong \frac{0.645x}{u_0}.$$

To complement the data on the pulsating motion near the jet boundaries, correlation measurements of pulsations of velocity and static pressure were carried out. The pulsations of static pressure were measured with the help of a special nozzle with built-in Endevco 8507 fast-response sensors. The measurement procedure and conditions are described in [26]. The jet velocity at the nozzle exit was about 40 m/s, and the nozzle diameter was 190 mm.

Figure 5 shows the results of measurements of the correlation coefficients for velocity pulsations (measured with a thermoanemometer) and static pressure pulsations at a distance of 200 mm from the nozzle exit. The static pressure sensor was located in the middle of the mixing layer at the level of the nozzle edge. The measurements were carried out at different positions of the thermoanemometer sensor moved along the normal to the jet axis.

Figure 5a shows an example of the correlation dependences of the transverse velocity and pressure pulsations in the form of time dependences of the correlation coefficient at different positions of the thermoanemometer sensor. Figure 5b shows the maximum values of the correlation coefficients determined by measurements of the longitudinal, u, and vertical, v, velocity components for different positions of the thermoanemometer sensor. The coordinate corresponding to the outer boundary of the jet, $y \approx 0.16x$, is also shown.

It can be seen that the maximum correlation between pulsations of the inflow velocity to the jet and static pressure pulsations in the jet is observed beyond the jet boundaries. These data correspond to the earlier results on the occurrence, in the pulsating motion beyond the jet, of periodic components induced by the motion of large-scale static pressure inhomogeneities, caused by the intermittency in turbulence.

The form of the correlation functions in Fig. 5a indicates the presence of a certain time scale in the process under consideration. Figure 6 shows the values of this scale obtained from measurements similar to those presented in Fig. 5 in different cross sections of the jet. The time scale was defined as the doubled dis-

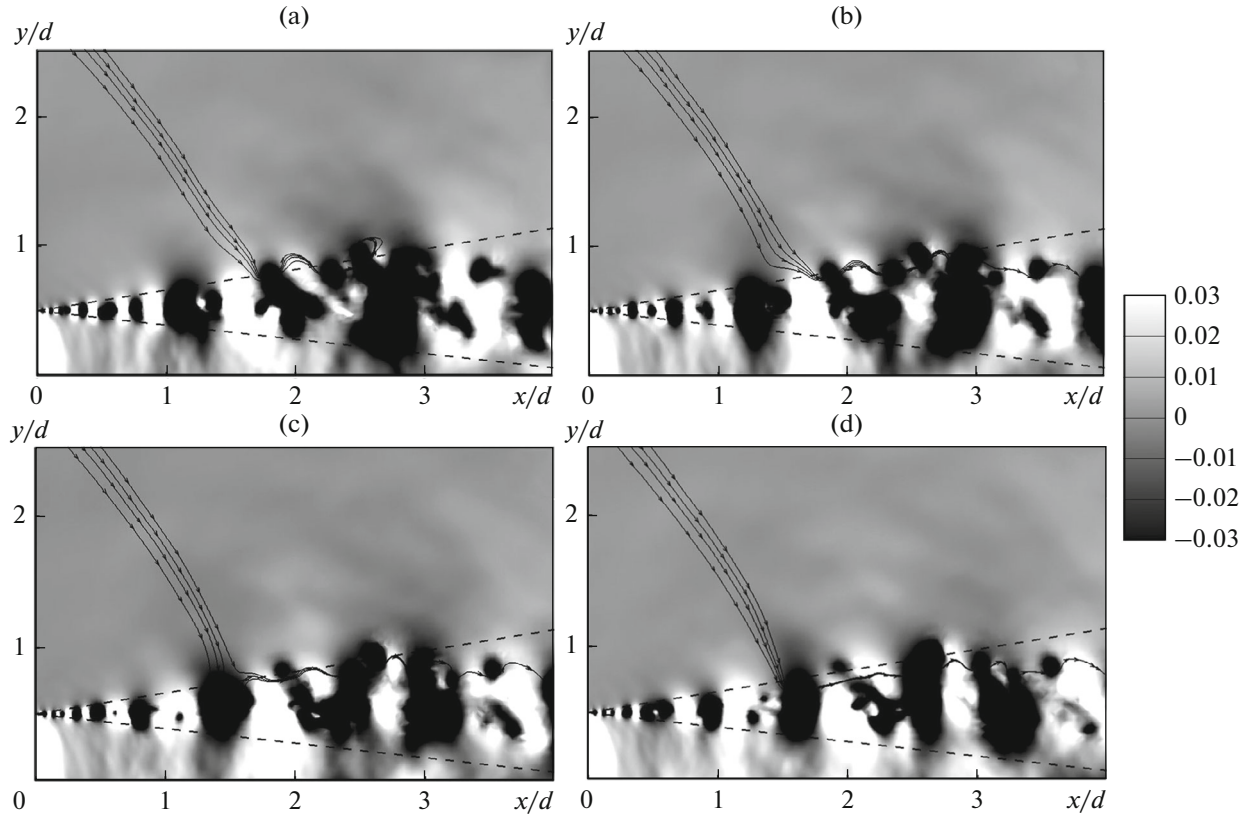

Fig. 4. Instantaneous flow patterns with separate streamlines.

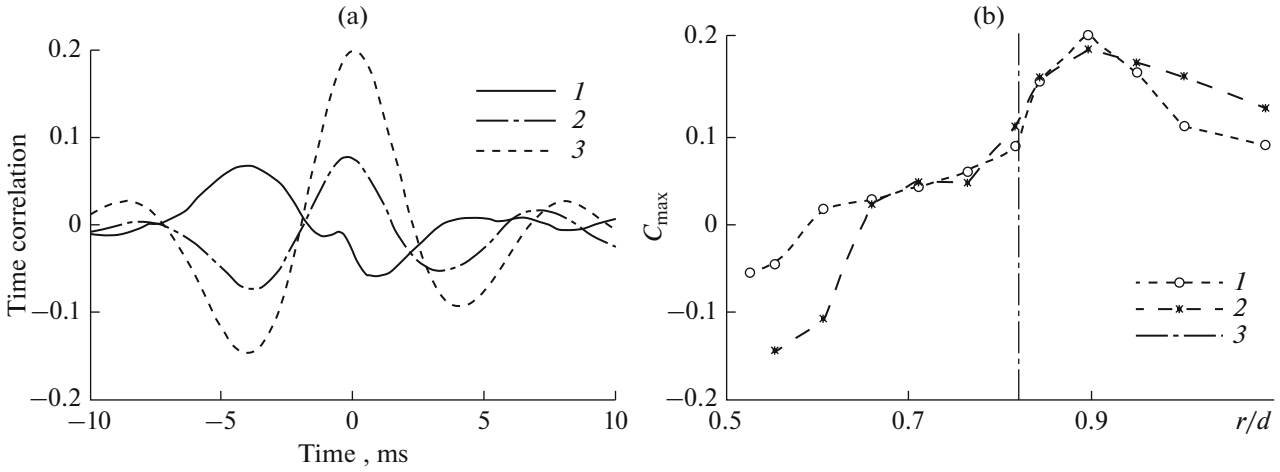

Fig. 5. (a) Intercorrelations of pressure pulsations in middle of mixing layer and longitudinal velocity pulsations at r/d = (*1*) 0.9, (*2*) 0.82 (2), and (*3*) 0.53 (3). (b) Maximum correlation vs. distance to jet axis: (*1*) u', (*2*) v', and (*3*) outer boundary of jet.

tance between the maximum and first minimum of the correlation dependences for the velocity pulsations outside the jet and pressure pulsations in the middle of the mixing layer. In Fig. 6, the symbols represent the results of measurements and the line corresponds to dependence (1): $\mathrm{Sh}_d = fd/u_0 = 1.55d/x$. These data are consistent with the fact that, near the jet boundaries, periodic perturbations are created with a radiation frequency corresponding to the experimental and calculated data on the location of noise sources of turbulent jets.

Similar data are available for swirling jets with a high swirling intensity. In [2, 23, 24], the results of studies of swirling jets with a swirling intensity $W_0 \geq 1$ are presented

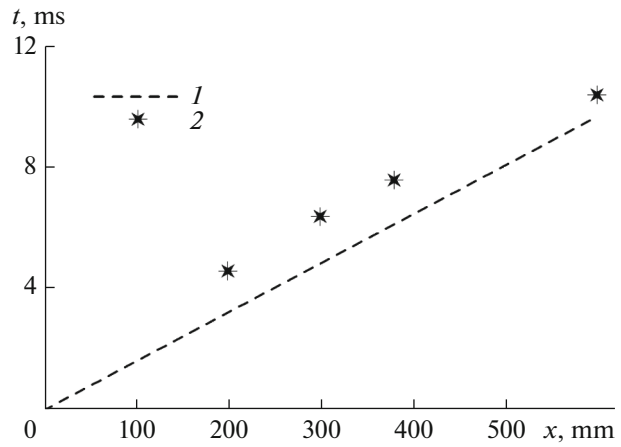

Fig. 6. Time scale determined from correlation of velocity outside jet and pressure in middle of mixing layer: (*1*) $\mathrm{Sh}_d = 1.55d/x$ and (*2*) experiment.

when a zone of recurrent flow in the near-axis region arises. Due to the presence of tonal radiation from the jet, the periodic signal of this radiation was used as the base signal for time calculating in the analysis of changes in the structure of the averaged flow in the jet.

According to the results of measurements, the distribution of dynamic parameters (the averages for the phase realizations) rotates (precesses) in the jet cross section virtually as a whole according to the law of rotation of a rigid body. The frequency of this rotation is equal to the first, fundamental frequency of tonal radiation.

It was shown in [23, 24] that precession in a swirling jet is accompanied by a virtually "frozen" rotational motion of the distributions of the static pressure and other parameters in the cross section of the jet. The circular displacement of the static pressure inhomogeneity causes periodic perturbations in the flow structure in the jet.

According to [26], the streamlines of the external flow, just like in Fig. 3 in the case of an ordinary jet, are entrained in the precessional motion of the depressed region in a swirling jet and also exhibit return motion with significant rotation of the flow structure due to precession. The period of this motion is equal to the period of precession and corresponds to the frequency of tonal sound radiation.

In the case of a swirling jet, as in the case of a turbulent jet, a sharp movement in the surrounding medium in the return movement of the streamlines is observed. These pulsations apparently give rise to acoustic waves.

The data confirm the presence of quasi-periodic perturbations in the external flow induced by jets, disturbing its uniformity.

RESULTS OF NUMERICAL CALCULATION AND EXPERIMENTS ON DETERMINING THE PHASE CHARACTERISTICS OF VELOCITY AND PRESSURE PULSATIONS

In a swirling jet, acoustic radiation is produced [2, 27], the fundamental tone of which is determined by the swirling intensity W_0:

$$\mathrm{Sh}_w = fd/u_0 \cong 0.7w_0, \qquad (6)$$

where f is the frequency, d is the nozzle diameter, $w_0 = w_m/u_0$, u_0 is the mean efflux velocity, and w_m is the maximum value of the rotational velocity component (at the nozzle exit).

In [23, 24], detailed results of the study of a swirling jet with $w_0 \cong 1.7$ were presented. The flow structure and the characteristics of velocity and pressure pulsations were determined. The measurements showed that the phase difference between the radial velocity and pressure pulsations varies in the jet flow from 0° to 360°. Figure 7 shows the results of measuring the phase ratio outside the jet. The velocity and pressure pulsation phases (φ) are presented at different distances from the jet along the normal to axis r, calculated from the nozzle edge; the x axis is the ratio r/λ, where λ is the wavelength of tonal sound. The phase difference Δφ decreases with increasing r and passes through a value of $\Delta\varphi = 90°$ at $r/\lambda \approx 0.03$. Starting from this value of r, the phases of pressure and radial velocity pulsations become close and, at $r/\lambda \approx 0.28$, coincide, which corresponds to the end of sound wave generation. These data indicate (1) the absence of a pulsation energy flux from the region of the jet flow and (2) the acoustic radiation generation in the range of Δφ from 90° to 0°. This agrees with the data of [23, 24, 26] on the periodic rearrangement of the inflow into the jet.

To study the processes of noise generation by an ordinary turbulent jet, in contrast to phase analysis in the case of a swirling jet, we separated the specific frequencies by the method described in [14]. Calculations based on the solution to three-dimensional time-dependent Navier–Stokes equations for a compressible medium require significant computer resources and special processing of the results, which comprise a large number of data sets. The calculations used spatial meshes with approximately 3×10^6 nodes. The calculations were performed with relaxation within a time interval of 10^{-4} s for ten iterations and with accumulation of data for approximately 1 s.

It should be noted that, due to the large amount of processed data, we had to limit their representation to their part least dependent on the calculation error caused by the limitation of the amount of calculations and insufficient accuracy associated with the specifics in calculating very small deviations of such parameters as density, pressure, temperature, pulsation phase, etc.

The time variation in the phases of velocity and pressure pulsations at different frequencies (Sh = var)

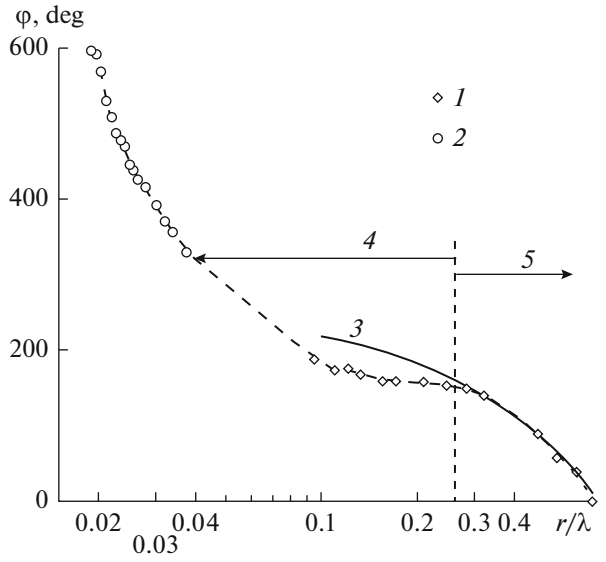

Fig. 7. Measured phases of pressure and velocity pulsations near swirling jet: (*1*) phase of pressure, (*2*) phase of velocity, (*3*) $\varphi = \text{const}\, fr/a_0$, (*4*) transient region, and (*5*) acoustic field.

was studied. The nonstationary spatial distribution of the radiation phase was obtained by the method described below by accumulating the pressure values at each time step during the calculation in a selected cross section. As a result, at each point of the section, the realization $P_{i,j}(t_n)$ of pressure (or the velocity component) is stored, where i and j are the indices of the point, $t_n = t_0 + n\Delta\tau$ is time, $n = 0,..., N-1$ is the time index, N is the number of time steps stored, t_0 is the start time of saving the data, and $\Delta\tau$ is the time step.

Then, for each time point t_n, we can construct a discrete Fourier transform (DFT):

$$X_{i,j}(k) = \sum_{l=n}^{n+\Delta n} P_{i,j}(t_l) e^{-i\frac{2\pi}{T}k(l-n)},$$
$$k = 0,\ldots,\ \Delta n - 1,$$

were

k is the index of frequency;

l is the number of the time step;

Δn is the number of time steps processed;

$T = \Delta n \Delta\tau$ is the length of the time interval under study;

$X_{i,j}(k)$ is a set of complex amplitudes of sinusoidal signals;

$\arg(X_{i,j}(k))$ is the phase of the kth sinusoidal signal.

The index of frequency is related to the signal frequency as follows:

$$f = \frac{k}{T} = \frac{k}{\Delta n \Delta\tau}.$$

In our calculations, the DFT was calculated with an interval Δn of 1024 time steps. Then, e.g., the index of frequency $k = 16$ corresponds to the frequency $f = 156$, which roughly corresponds to the number Sh = 1 for the given problem.

Next, for each point of the cross section, for a time point t_n, we can calculate the pulsation phase at a given frequency. For Sh = 1,

$$\varphi^n_{i,j} = \arg(X_{i,j}(k = 16)).$$

After calculating the radiation phase for the entire cross section, the next time step $n = n + 1$ is chosen. As a result, for each point, we obtained a realization of the pulsation phase, $\varphi_{i,j}(t_n) = \varphi^n_{i,j}$, at a time point t_n, where $n = 0, ..., (N - \Delta n) - 1$. The DFT is calculated using fast Fourier transform. The use of an interval Δn twice as large or small gives qualitatively the same results but with a large number of distortions. The implementation of this technique records all perturbations in the flow region and at a given frequency.

Figure 8 shows the results of calculating the instantaneous phase distribution for a frequency of 156 Hz. Here and below, we present the results of numerical calculations of the formation and propagation of an acoustic perturbation for different Sh numbers from

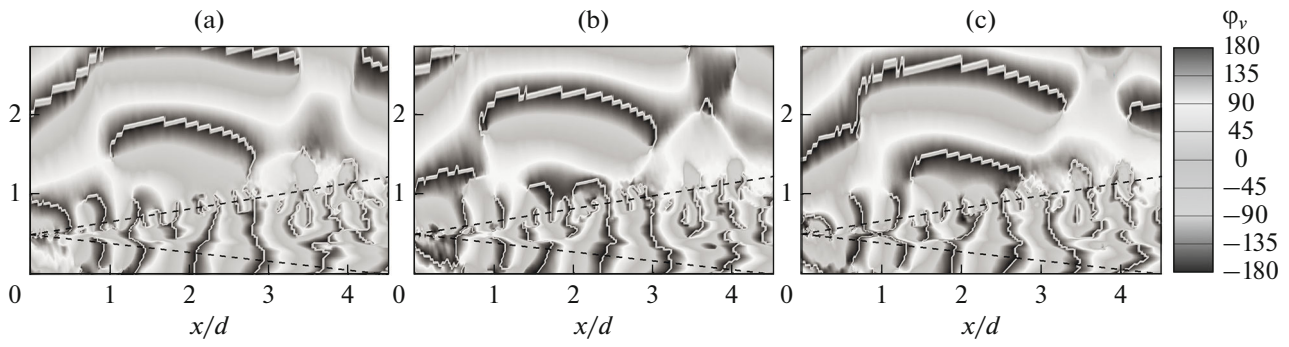

Fig. 8. Illustration of acoustic wave generation.

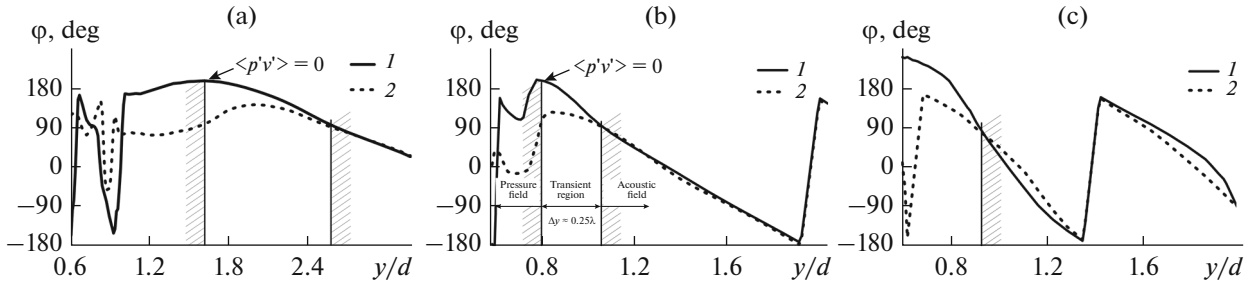

Fig. 9. Phase distribution for pressure and velocity pulsations in cross section of jet: Sh = (a) 0.5, (b) 1, and (c) 1.5: (*1*) pressure pulsations and (*2*) velocity pulsations. Values of x/d are given in text.

[13–15]. Figure 8 shows a sequence of phase distributions for vertical velocity pulsations after 1/3 of a period for Sh = 1 in the form of frames with instantaneous phases. The lines in which the velocity pulsations phases are 0° or 360° are shown, i.e., the lines characterizing the position of acoustic waves. The coordinates of the cross section in which, according to (1), the source of sound of this frequency is located is $x/d \cong 1.55$.

In the first frame, we can visually observe the initial location of the small area in which the acoustic wave emerges; its coordinates are $x/d \cong 1.55$, $y/d = 1.01$–1.04. Similar data were obtained for pressure pulsation. Starting from this vertical coordinate, the distance between lines of equal phase corresponds rather accurately to the wavelength with a frequency $f = 156$ Hz. It is possible to confirm this observation by comparing the phase distributions for velocity and pressure pulsations for fixed frequencies along the vertical coordinate at the time point corresponding to the first frame in Fig. 8.

Figure 9b shows the values of the phase of velocity and pressure pulsations for Sh = 1 and $x/d \cong 1.55$ along the vertical line. These data indicate that, for $y/d < 0.8$, the phase difference exceeds 90° and is equal to zero starting from $y/d \cong 1.04$. A possible explanation for this is that an acoustic wave is formed in the region between these values of the transverse coordinate.

Similar data were obtained for other cross sections of the jet: Sh = 0.5, $x/d \cong 3.1$ and Sh = 1.5, $x/d \cong 1.05$ (Figs. 9a and 9c, respectively). These data show that the generation of acoustic waves at fixed frequencies takes place outside the mixing zone, in the region where the coordinate y exceeds $y_2(x)$, which, in the traditional flow pattern in the jet (Fig. 1), separates the mixing zone from the ambient space.

The phase difference Δφ between the velocity and pressure pulsations characterizes the direction in which perturbations propagate and the magnitude of the energy flux in the direction of velocity v [5]. The correlation is

$$\langle p'v' \rangle = (\langle p'^2 \rangle \langle v'^2 \rangle)^{1/2} \cos(j). \qquad (7)$$

As Δφ approaches 90°, the energy transfer due to pulsation propagation decreases and its direction changes sign. The energy component of these perturbations depends on all three components in relation (7). Since, with increasing distance from the mixing zone, the maximum level of pulsations can only decrease, the increase in the acoustic energy flux at a fixed frequency from zero (at Δφ = 90°) to the final value can take place only due to the energy transfer from hydrodynamic to acoustic perturbations as the pulsations phases approach each other.

Thus, based on the data presented in Fig. 9, it can be assumed that the generation of acoustic waves takes place outside the mixing zone due to the inducement of pulsating motion in the inflow of the surrounding medium. The induced pulsation mechanism was described in the previous section.

It should be noted that the calculated data generally agree with relation (1), which determines the location of the sound source for a given frequency. When calculating the dependences of the pulsation phase characteristics on the transverse coordinate, the initial time and coordinate x/d were varied. The results of calculations showed that the best agreement with relation (1) is reached for Sh = 1.

For Sh = 1.5, the agreement can be considered satisfactory. For Sh = 0.5, according to visualization data similar to those shown in Fig. 8, the propagation of the acoustic wave originates at $x/d = 3.2$...3.3, which is somewhat larger than in (1). Limited computer capacity prevented a more thorough study.

In Fig. 10, the calculation results for a free turbulent jet are shown as the boundaries of different perturbation generation and propagation regions determined from these data. Along with the known data on the position of the boundaries of the mixing zone (y_1, y_2, b) (see Fig. 1b), Fig. 10 shows the boundaries of the supposed region (y_p and y_f) in which the phase difference between the transverse velocity and pressure pulsations for particular frequencies varies from 90° to zero.

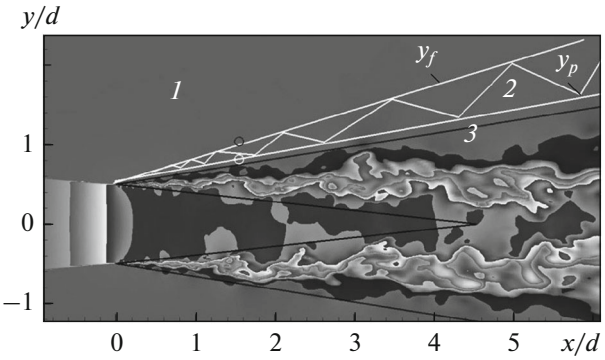

Fig. 10. Boundaries of characteristic zones for submerged turbulent jet: (*1*) acoustic field, (*2*) transient region, and (*3*) pattern of turbulent flow.

Figure 11 shows the same experimental data for a swirling jet in its cross section. Acoustic radiation forms in the region bounded by the dashed lines.

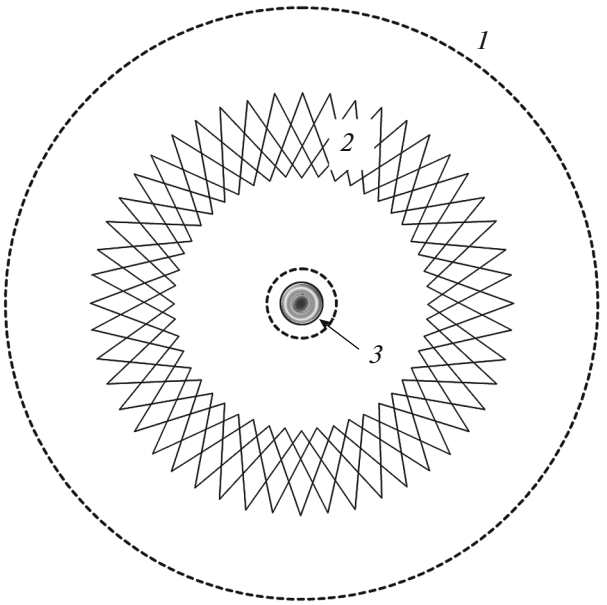

Fig. 11. Boundaries of characteristic zones for swirling jet: (*1*) acoustic field, (*2*) transient region, and (*3*) pressure field.

ON THE FORMATION OF THE SOURCE OF ACOUSTIC PERTURBATIONS

In a nonswirling turbulent jet, sound generation results from multiple periodic processes caused by the intermittent motion of large-scale inhomogeneities of the turbulent fluid: regions with reduced static pressure. It is expedient to consider this process of the hydrodynamic formation of acoustic waves compared to the formation of acoustic waves produced by periodic motion of a rigid body.

In [28], the results of a numerical calculation (based on the solution of the Euler equations) of acoustic radiation arising in an eccentric rotation of a cylinder at a given frequency are presented. The case was considered in which the size of the source is smaller than the wavelength of the acoustic radiation generated. As a result of the calculations, regularities of the acoustic wave generation were determined.

Near the cylinder, the phases of pressure and radial velocity pulsations in the propagating perturbations do not coincide and, with an approach to the surface of revolution formed by the boundary of the cylinder, the phase difference is slightly less than 90°. At a distance from the cylinder of approximately quarter the wavelength, the phases become closer and, in the propagating perturbations, correspond to acoustic waves. Nevertheless, the energy flux I in propagating perturbations does not change with distance from the cylinder:

$$I = \langle p'v' \rangle R = \text{const}, \qquad (8)$$

where R is the distance from the center. This means that the energy of propagating perturbations is generated in a thin layer in the immediate vicinity of the source.

Above, we have presented the results of studies on acoustic wave generation by nonstationary motion of a fluid or gas.

In the case of turbulent jets, the characteristic sizes of inhomogeneities of a flow in which propagating acoustic perturbations of fixed frequency are formed can be determined from the data obtained from determining the velocity and pressure pulsation phases. These data are presented in Figs. 8–10. For fixed frequencies, the onset of the formation of periodic acoustic perturbations propagating from the mixing layer corresponds to $\langle p'v' \rangle = 0$, i.e., to a phase difference of 90°.

For example, let us consider sound formation in a jet with Sh = 1. According to the data in Figs. 8–10, this corresponds to $y/d \cong 0.81$. Under the condition that the acoustic energy flux I for a given frequency is conserved, by analogy with (8), the quantity $\langle p'v' \rangle R =$ const could also be conserved provided that the distance from the source is measured from the coordinate of its center, r_0. In this case, $r_0 = 0.81d$.

If we assume that, initially, the sound propagates normally to the jet axis, then $R = y - r_0$. We can use these simplified representations to analyze the computer simulation data presented in Figs. 9 and 10. They were obtained for a fixed radiation frequency Sh = 1 ($f =$ 156 Hz), for which the radiation source was located at $x/d \approx 1.51$. According to these data, the propagation of acoustic perturbation for a jet efflux velocity of 310 m/s can begin to be seen (Fig. 8) at $y/d = 1.1$; for the same value of the coordinate (Figs. 9 and 10), the pulsation phases p' and v' become equal.

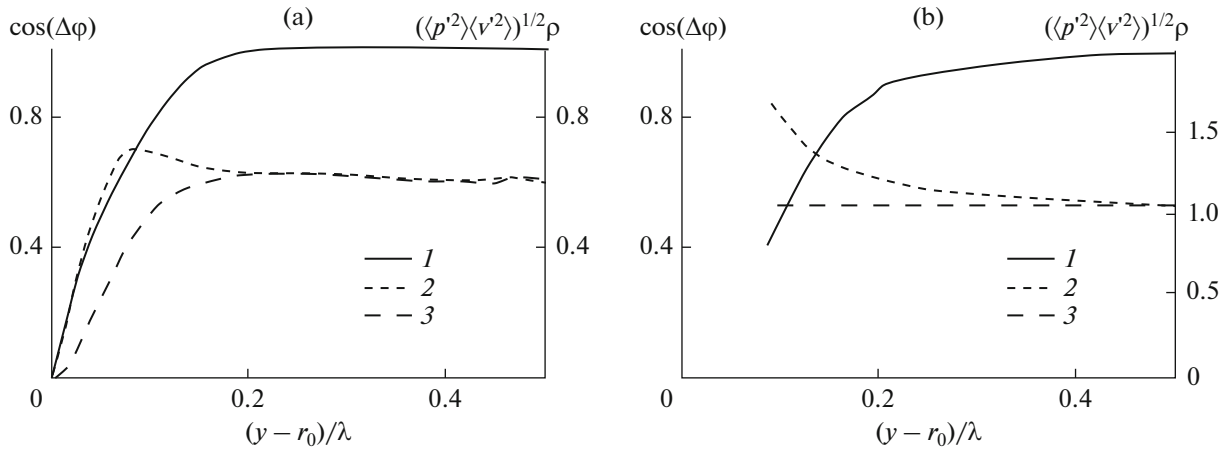

Fig. 12. Distribution of quantities $\langle p'v'\rangle$ and $\langle p'v'\rangle\rho$: (a) over radius for free jet at $x/d = 1.55$ (Sh = 1) and (b) for rotating cylinder: (*1*) cos(Δφ) (left scale) and ρ = (*2*) R/λ and (*3*) $\cos(\Delta\varphi)R/\lambda$ (right scale).

At the same time, the onset of formation of acoustic perturbations takes place at $r_0 = 0.81d$.

To verify this scheme of the conditional sound source, the data on the parameters of propagating perturbations in the case of a jet and a rotating cylinder were combined in Figs. 12a and 12b. They present the dependence of $\langle p'v'\rangle$ and $\langle p'v'\rangle$ R on the distance measured from the center of the source, determined from (7). For a turbulent jet, the x axis is $(y - r_0)/\lambda$ and, for a rotating cylinder, R/λ. (The λ value for the jet was determined from relation (3).) It can be seen that, in the latter case, relation (8) is satisfied with satisfactory accuracy. Figure 12 presents a comparison of the dependences cos(Δφ), where Δφ is the phase difference between the of velocity and pressure pulsations, on the transverse coordinate for a jet and a rotating cylinder (Figs. 12a and 12b, respectively).

The similarity of the dependences characterizing the variation in the phase difference between the velocity and pressure pulsations (cos(Δφ)) confirms the earlier conclusion on the determining parameter for the sizes of the region of acoustic emission generation: approximately a quarter wavelength.

On the other hand, the data in Fig. 12, which presents the results of determining the acoustic energy fluxes by (8), indicate a fundamental difference between the processes of energy transfer from pulsating motion to acoustic pulsations in the case of sound generation by pulsating motion of a rigid body and pulsating motion of a liquid or gaseous medium.

When comparing other data in Fig. 12 for $R/\lambda > 0.2$, it can be seen that, starting from some distance from the source, relation (8) for the jet is satisfied just as it is certainly satisfied for the cylinder. In other words, in a certain region, the propagation of acoustic perturbations from a jet is similar to the propagation of perturbations from a cylindrical source. (However, the computation data show that, at distances greater than shown in Fig. 12a, this dependence is violated.)

The data in Figs. 9–12 show that, with increasing distance from the jet axis, the direction in which perturbations propagate undergoes changes. Starting from the jet boundary y_2, large velocity and pressure perturbations existing in the mixing layer are not detected. Near the jet boundary, at $y = y_p \approx y_2$, the phase difference of perturbations for the characteristic radiation frequencies (1) is 90°, the correlation is $\langle p'v'\rangle = 0$, and the energy flux of pulsation motion outward is absent. Only the presence of pulsations in the flow induced by the jet provides energy for the generation of these quasi-periodic acoustic pulsations.

According to the ideas set forth in [30, 31], hydrodynamic pulsations give rise to acoustic pulsations "because of the interaction of the field of velocity pulsations with themselves." These pulsations, propagating from the jet, receive energy from the pulsating motion of the inflow. Their intensity reaches the final level at a distances at which the induced pulsating motion in the inflow has completely weakened. This process is illustrated by the data of phase measurements (Figs. 9–11).

For $y \approx y_2$, the value of cos (Δφ)—the phase difference between the pulsation velocity and pressure—is zero. With increasing distance from the jet boundary, this value approaches unity; i.e., for the frequencies under consideration, the energy component of propagating pulsations gradually increases, although the intensity of velocity pulsations decreases (Fig. 12).

These data allow us to limit the region containing some conditional sources of perturbations. Their characteristic frequencies correspond to relation (1). A scheme of this region is shown in Fig. 10. The outer boundary of this region may be the $y = y_f$ value at which $\Delta\varphi \approx 0$, i.e., when the perturbations become

purely acoustic. As for the initial position of the conditional source, it is located closer to the mixing layer; this position is shown in Fig. 10 roughly between y_p and y_f. The characteristic size of the region between the boundaries y_p and y_f can depend on two characteristic sizes of the process under consideration: L and λ. According to Figs. 7–12, it approximately corresponds to a quarter wavelength of the radiation generated.

CONCLUSIONS

The results of this study can be interpreted as follows. The formation of acoustic radiation or noise generation in jets, although caused by nonstationary processes in areas commonly referred to as jet flow regions, can occur outside these regions due to the energy of pulsations induced in the inflowing medium. The region where these pulsations occur is usually called the near acoustic field of the jet, which in this case can be considered a source of acoustic radiation.

Turning to Fig. 10, we can propose the following schematization of a jet flow: it is based on the scheme proposed by G.N. Abramovich, shown in Fig. 1. We added two new boundaries to it: y_p and y_f. The boundary y_p almost coincides with the outer boundary of the mixing layer, y_2. Here, acoustic radiation begins to form. The boundary y_f is the value of the transverse coordinate starting from which the phases of the propagating pressure and velocity pulsations coincide. The physical meaning of the region between y_2 and y_f is the near acoustic field of the jet. In the initial section of a turbulent jet, the position of the boundaries can be approximately considered linear in x.

According to the data obtained for a turbulent jet and a swirling jet, the distance between boundaries y_p and y_f approximately corresponds to a quarter wavelength of the acoustic radiation.

It is worth noting that the presented data are consistent with the ideas set forth in [16, 32, 33] on using chevrons or lobes to reduce jet noise under the action of longitudinal vorticity created in the source of the jet. According to [32], chevrons and lobes placed at the nozzle exit create vorticity in the outer part of the jet flow; in this case, the intensity of the noise emitted by the jet decreases approximately in proportion to the magnitude of the longitudinal vorticity created [16, 32]. Comparing the data of this study with the pattern of the inflow into the jet in the presence of chevrons from [33], we can conclude that the longitudinal vorticity affects the jet precisely in the region of sound generation.

The results of this study confirm the model of noise generation in turbulent jets formulated at the beginning of this paper. However, the results obtained have not shown a direct relation of the acoustic field observed experimentally and calculated numerically with basis LES technology with the data from analysis of pulsating motion in a jet. The justification is that the characteristics of the far field and the pulsation characteristics of the flow are obtained in the same calculation, and they are confirmed by the experimental data on individual properties of a jet flow.

To validate our conclusions, they must be supported by an analysis of the integral acoustic power emitted at the selected frequencies. To do this, it is necessary to show that the acoustic radiation energy produced in periodic processes in the near field of the jet, starting from a certain distance, ceases to change and corresponds to the far field characteristics.

The basic ideas about the noise generation process in a turbulent flow are contained in Lighthill's model of noise generation by turbulent jets [1]. According to this model, the acoustic energy flux I emitted by a jet is determined by a relation that can be represented as follows:

$$I(x) = \frac{x_i x_j x_k x_l}{16\pi^2 a^5 x^6 \rho} \times \iint \left\langle \left[\frac{\partial^2}{\partial t^2} (T_{ij} - \langle T_{ij} \rangle) \right] \left[\frac{\partial^2}{\partial t^2} \left(T'_{kl} - \left\langle T'_{kl} \right\rangle \right) \right] \right\rangle dy dy',$$

$$T_{ij}(y) = \rho u_i u_j + P_{ij} - a^2 \rho \delta_{ij},$$

$$P_{ij} = p\delta_{ij} + \eta \left[-\frac{\partial u_i}{\partial x_i} - \frac{\partial u_i}{\partial x_i} + \frac{2}{3} \left(\frac{\partial u_k}{\partial x_k} \right) \delta_{ij} \right],$$

where the angular brackets denote time averaging, x is the distance to the source, ρ is density pulsation in the acoustic wave, p is pressure, u_i and u_j are the velocity components, η is the molecular viscosity, ρ is the density, and a is the speed of sound in the surrounding medium. It is usually assumed that the integration region is the mixing layer, i.e., the region between boundaries y_1 and y_2. The data of this study show that integration should be performed over the region usually considered the near acoustic field of the jet. Such an analysis could confirm these conclusions or require new research. At the same time, the corresponding calculations require significant efforts, as well as the development of computing technologies.

ACKNOWLEDGMENTS

This work was supported by the Russian Foundation for Basic Research, project no. 17-01-00213a.

REFERENCES

1. M. J. Lighthill, Proc. R. Soc. London, Ser. A **221** (1107), 564 (1952).
2. *Turbulent Mixing of Gas Jets,* Ed. by G. N. Abramovich (Nauka, Moscow, 1974) [in Russian].
3. G. N. Abramovich, *Theory of Turbulent Jets* (Nauka, Moscow, 1984) [in Russian].

4. A. G. Munin, V. M. Kuznetsov, and E. A. Leont'ev, *Aerodynamical Noise Sources* (Mashinostroenie, Moscow, 1981) [in Russian].
5. L. K. Zarembo and V. A. Krasil'nikov, *Introduction into Nonlinear Acoustics* (Nauka, Moscow, 1966) [in Russian].
6. *Aviation Acoustics,* Ed. by A. G. Munin and V. E. Kvitka (Mashinostroenie, Moscow, 1973) [in Russian].
7. S. Yu. Krasheninnikov and A. K. Mironov, Fluid Dyn. **45** (3), 402 (2010).
8. C. Tam and L. Aurialt, AIAA J. **37** (2), 145 (1999).
9. P. Morris and S. Boluriaan, in *Proc. 10th AIAA/CEAS Aeroacoustics Conference* (Manchester, 2004), Paper No. AIAA-2004–2977.
10. C. Tam, K. Viswanathan, K. Ahuja, and J. Panda, J. Fluid Mech. **615**, 253 (2008).
11. V. F. Kopiev, I. V. Belyaev, M. Yu. Zaytsev, V. A. Kopiev, and G. A. Faranosov, Acoust. Phys. **59** (1), 19 (2013).
12. A. Guitton, F. Kerheve, P. Jordan, and J. Delville, in *Proc. 14th AIAA/CEAS Aeroacoustics Conference* (Vancouver, 2008), Paper No. AIAA-2008-2892.
13. S. Yu. Krasheninnikov and L. A. Benderskii, in *Proc. All-Russian Convention on Fundamental Problems on Theoretical and Applied Mechanics* (Kazan, August 20–24, 2015), p. 2073.
14. L. A. Benderskii and S. Yu. Krasheninnikov, Fluid Dyn. **51** (4), 568 (2016).
15. L. A. Benderskii, S. Yu. Krasheninnikov, and A. K. Mironov, in *Proc. 6th All-Russian Conference "Computational Experiment for Acoustics"* (Svetlogorsk, September 19–24, 2016).
16. S. Yu. Krasheninnikov and A. K. Mironov, Akust. Zh. **54** (3), 392 (2008).
17. M. J. Fisher, M. Harper-Bourne, and S. A. L. Glegg, J. Sound Vib. **51** (1), 23 (1977).
18. G. R. Mac-Gregor and C. D. Simcox, in *Proc. AIAA Aeroacoustics Conference* (Seattle, WA, 1973), Paper No. AIAA 73-1041.
19. *High Velocity Jet Noise Source Location and Reduction, Report No. FAA-RD-76-79* (US Department of Transportation, Federal Aviation Administration, Washington, DC, 1977).
20. A. K. Mironov, S. Yu. Krasheninnikov, V. P. Maslov, and D. E. Zakharov, Acoust. Phys. **62** (4), 483 (2016).
21. H. K. Lee and H. S. Ribner, in *Proc. AIAA 5th Fluid and Plasma Dynamics Conference* (Boston, MA, 1972), Paper No. AIAA 72-640.
22. M. Schaffar, J. Sound Vib. **64** (1), 73 (1979).
23. S. Yu. Krasheninnikov, A. K. Mironov, D. E. Pudovikov, and P. D. Toktaliev, Fluid Dyn. **50** (3), 371 (2015).
24. D. L. Zakharov, S. Yu. Krasheninnikov, V. P. Maslov, A. K. Mironov, and P. D. Toktaliev, Fluid Dyn. **49** (1), 51 (2014).
25. L. A. Benderskii and D. A. Lyubimov, Uch. Zap. TsAGI **45** (2), 22 (2014).
26. L. A. Benderskii, S. Yu. Krasheninnikov, and A. K. Mironov, Fluid Dyn. **52** (6), 759 (2017).
27. S. Yu. Krasheninnikov, Izv. Akad. Nauk SSSR, Mekh. Zhidk. Gaza, No. 6, 148 (1971).
28. S. Yu. Krasheninnikov, A. K. Mironov, D. E. Pudovikov, and K. S. P'yankov, in *Proc. 3rd All-Russian Open Conference on Aviation Acoustics* (Zvenigorod, 2013), p. 40.
29. O. V. Yakovlevskii and A. N. Sekundov, Izv. Akad. Nauk SSSR, Mekh. Mashinostr., No. 3, 39 (1964).
30. A. S. Monin and A. M. Yaglom, *Statistical Hydromechanics. Mechanics of Turbulence* (Nauka, Moscow, 1967), Part 2 [in Russian].
31. L. D. Landau and E. M. Lifshits, *Course of Theoretical Physics,* Vol. 6: *Fluid Mechanics* (Pergamon Press, Oxford, 1987; Nauka, Moscow, 1986).
32. S. Yu. Krasheninnikov and A. K. Mironov, Izv. Akad. Nauk, Mekh. Zhidk. Gaza, No. 5, 43 (2003).
33. I. A. Brailko and S. Yu. Krasheninnikov, Izv. Akad. Nauk, Mekh. Zhidk. Gaza, No. 2, 76 (2005).

Translated by E. Chernokozhin